Simultaneous multi-slice imaging reduces sensitivity of local-SAR to patient motion at 7T

Emre Kopanoglu [1], Cem M. Deniz [2], Richard G. Wise [1,3]

[1] Cardiff University Brain Research Imaging Centre (CUBRIC), School of Psychology, Cardiff University, Cardiff, UK

[2] Department of Radiology, New York University School of Medicine, New York, NY 10016 USA

[3] Institute for Advanced Biomedical Technologies, Department of Neuroscience, Imaging and Clinical Sciences, G. D'Annunzio University of Chieti-Pescara, Chieti, Italy

Synopsis

This study investigates the effect of within-scan patient motion on local-SAR for simultaneous multi-slice (SMS) imaging at 7T. A virtual body model was simulated at 104 different positions. 1-/2-/3-spokes pulses were designed to excite a region of 60 slices covering the cerebellum and the brain, using SMS-factors of 1 through 5. Local-SAR was observed to increase by up to 2.75-fold due to patient motion. Pulses with higher SMS-factors were up to 50% less sensitive against changes in local-SAR due to patient motion, compared to SMS:1 pulses. Pulses with higher SMS-factors yielded more consistent local-SAR throughout the scan.

Summary of main findings

- Simultaneous multi-slice (SMS) pulses with higher SMS-factors are more robust against local-SAR changes due to patient motion.

- Pulses with higher SMS-factors yield more consistent local-SAR throughout the scan.

- A maximum local-SAR increase of 2.75-fold was observed due to patient motion.

Purpose

To investigate the effect of within-scan patient motion on the local specific absorption (SAR) rate for simultaneous multi-slice imaging at 7T.

Introduction

Simultaneous multi-slice (SMS) imaging has been increasingly used in brain imaging (1). At ultrahigh field (UHF), SMS is combined with parallel transmit (pTx) pulses to provide uniform excitations in multiple slices/slabs while reducing the total scan time through the acceleration provided by SMS (2,3). To control local-SAR, computational models are commonly used in pTx pulse design for UHF imaging (4).

For single-slice pTx pulse optimization, it was shown that within-scan patient motion can cause local-SAR to increase by up to 3.1-fold (5). As the utilization of SMS imaging with pTx pulses is expected to grow in the future, in this study, we investigate changes in local-SAR due to within-scan patient motion when SMS pTx pulses are employed.

Methods

The virtual body model Ella (IT'IS Foundation, Zurich, CH)(6) was simulated in Sim4Life (Zurich MedTech,Zurich, CH) at 104 different relative positions inside a generic 8-channel parallel transmit array (Figure 1). These positions covered all six degrees-of-freedom of motion as well as off-axis

motion on axial and coronal planes. Translations of 1,2,5,10,15,20 mm along right or inferior, 1,2,5,10 mm along posterior (range limited due to geometrical constraints); and rotations of ±1,±2,±5,10,15,20 degrees in pitch, 1,2,5,10,15,20 degrees in roll, and ±1,±2,±5,±10,±15,±20 degrees in yaw were simulated (5). The body model consisted of 73 different tissues and the shoulders were included in the computation domain (7). The vectorized body model was discretized at an isotropic resolution of 2 mm.


(a)

(b)

(c)
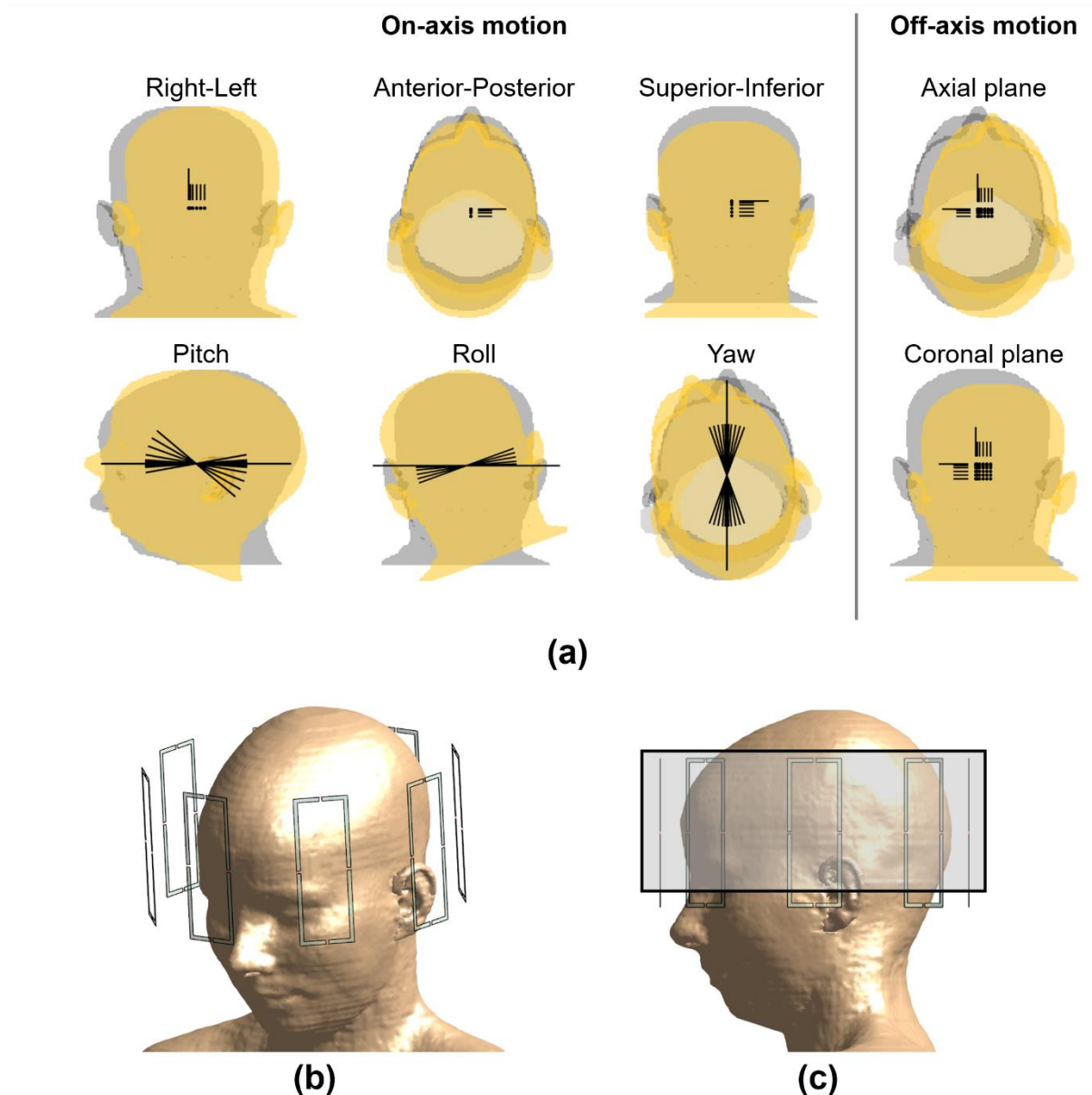
Figure 1: Simulation setup. (a) All six degrees-of-freedom of motion were simulated including off-axis displacement in axial and coronal planes. (b) The virtual body model was simulated inside a generic 8-channel parallel transmit array at 300 MHz. The simulation domain included the shoulders as recommended in the literature (7). (c) Simultaneous multi slice excitation pulses were designed for 60 slices covering the cerebellum and the brain, for SMS factors of 1 through 5, and for 1-, 2- and 3-spokes. The box indicates the coverage of the excited slices.

Using the simulated fields at the centred position, 1-spoke (RF-shimming), 2-spokes and 3-spokes slice selective RF pulses were designed to excite 60 axial slices (slice-thickness: 1.8 mm) that span the cerebellum and the brain (Figure 1c). The cost function was defined as the sum of normalized root-mean-squared error in the magnitude excitation profile (to enable phase relaxation) and the RF

power, the latter regularized by a Tikhonov parameter (8). The Tikhonov parameter was determined using an l-curve analysis. Spoke locations that minimize the cost function were individually selected for each designed pulse using the matching pursuit-guided-conjugate gradient method (9). Pulses were designed for interleaved simultaneous multi-slice (SMS) factors of 1 through 5 (e.g., first SMS:3 pulse excited slices 1-21-41).

A total of 411 pulses were designed (60,30,20,15,12 for SMS:1,2,3,4,5, respectively, for 1-/2-/3-spokes). The sensitivity of each pulses to patient motion was investigated by comparing their local-SAR at the off-centre positions to their local-SAR values at the centred positions. The ratio of the off-centre peak local-SAR values to the values at the centre are reported. Regions with higher local-SAR at the off-centre position than the peak local-SAR at the centred position are also compared for SMS:1 and SMS:5 cases for the worst-case positions for 2-spokes pulses. Pulses were also compared in terms of how the peak local-SAR changes throughout the scan.
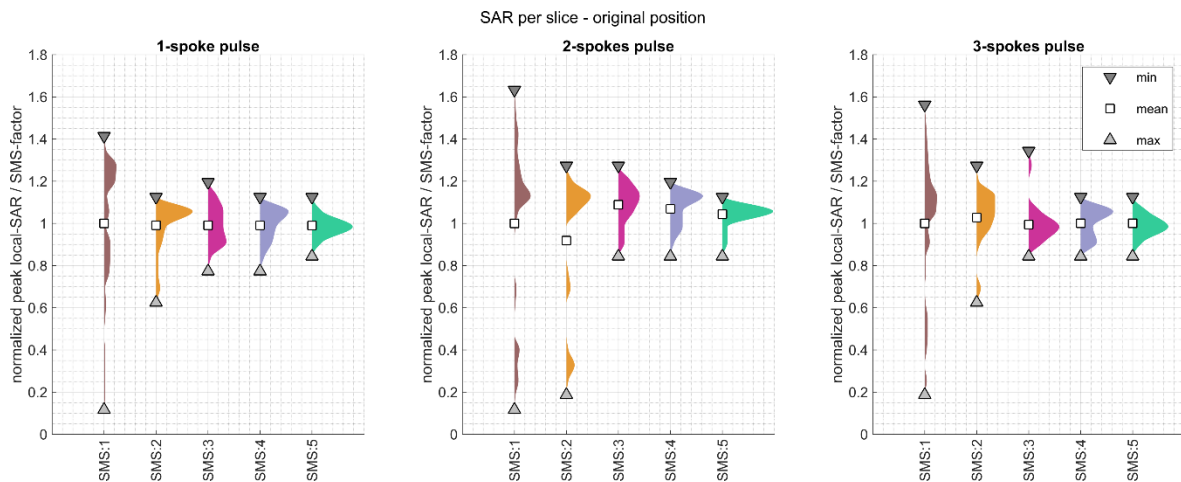
Figure 2: The variation of peak local-SAR across the pulses for different number of spokes and SMS-factors. All values were normalized by a) the SMS-factor as local-SAR inherently increases with the SMS-factor, and b) the scan-averaged peak local-SAR of their respective SMS:1 case. Using higher SMS-factors reduces the variation of peak local-SAR across pulses, leading to more consistent local-SAR values throughout the scan. Violin plots indicate the relative frequency of occurrence of a peak local-SAR value.

Results

SMS:1 pulses yielded a wide range of peak local-SAR values across the slices. For all pulses (1-/2-/3-spokes), increasing the SMS-factor reduced the variation of peak local-SAR across different slices/slice-groups and led to more consistent instantaneous peak local-SAR throughout the scan (Figure 2).

Increasing the SMS-factor reduced the sensitivity of local-SAR to patient motion. Patient motion led to up to 2.75-fold increase in peak local-SAR for 2-spokes SMS:1 pulses (Figure 3). Increasing the SMS-factor to 3 and above reduced the sensitivity to motion approximately by half as the maximum increase in peak local-SAR was around 1.4-fold for the higher SMS-factors (Figure 3). A similar behaviour was observed for 3-spokes pulses as well, with SMS:4 and SMS:5 reducing motion sensitivity by 50% compared to SMS:1 by reducing the maximum peak local-SAR increase from 2.4-fold to 1.2-fold (Figure 4). The increase in local-SAR for 1-spoke pulses reduced gradually from 2.6-fold to 2.2-fold as the SMS-factor was increased (Figure 4).

Increasing the SMS-factor also reduced the size of the region exposed to higher local-SAR than estimated at the centred position. Figure 5 compares the SMS:1 and SMS:5 cases for the 2-spokes pulse at the worst-case position. Compared to the peak local-SAR at the centre, the SMS:1 case yielded a maximum of 2.75-fold increase with a volume of 264 cm^3 exposed to higher SAR. For the

SMS:5 case, the volume exposed to higher SAR reduced by 88% to 32 cm^3, and the maximum increase was 39%.

Variation of instantaneous local-SAR with motion for all slices and positions
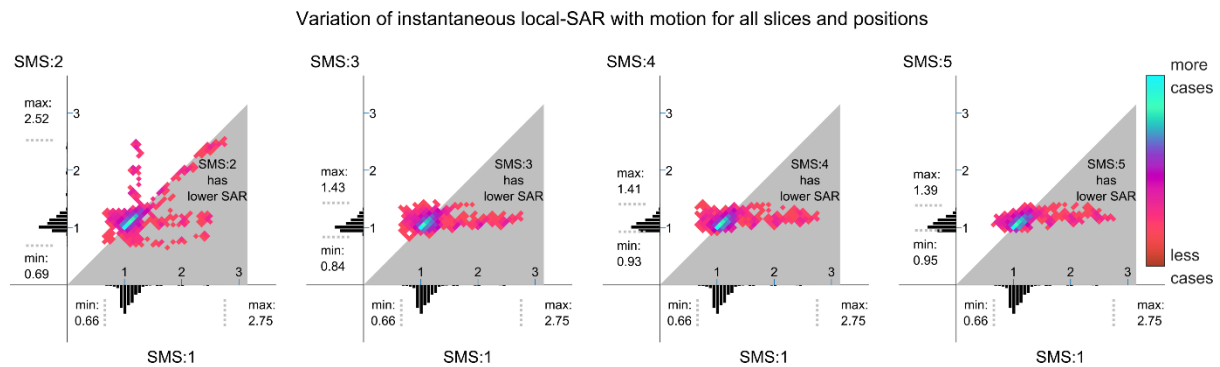
Figure 3: *The variation of peak local-SAR due to motion across all off-centre positions and all pulses is compared for different SMS-factors for 2-spokes pulses. The peak local-SAR at the off-centre positions were normalized with the respective peak local-SAR at the centre. For SMS:1, patient motion can cause up to 2.75-fold increase in the peak local-SAR, whereas increasing the SMS-factor to 5 reduces the motion-sensitivity approximately by half and the maximum increase is 1.39-fold. Intensities: number of cases that fall inside the patches. Histograms: projections onto the axes.*

Variation of instantaneous local-SAR with motion for all slices and positions
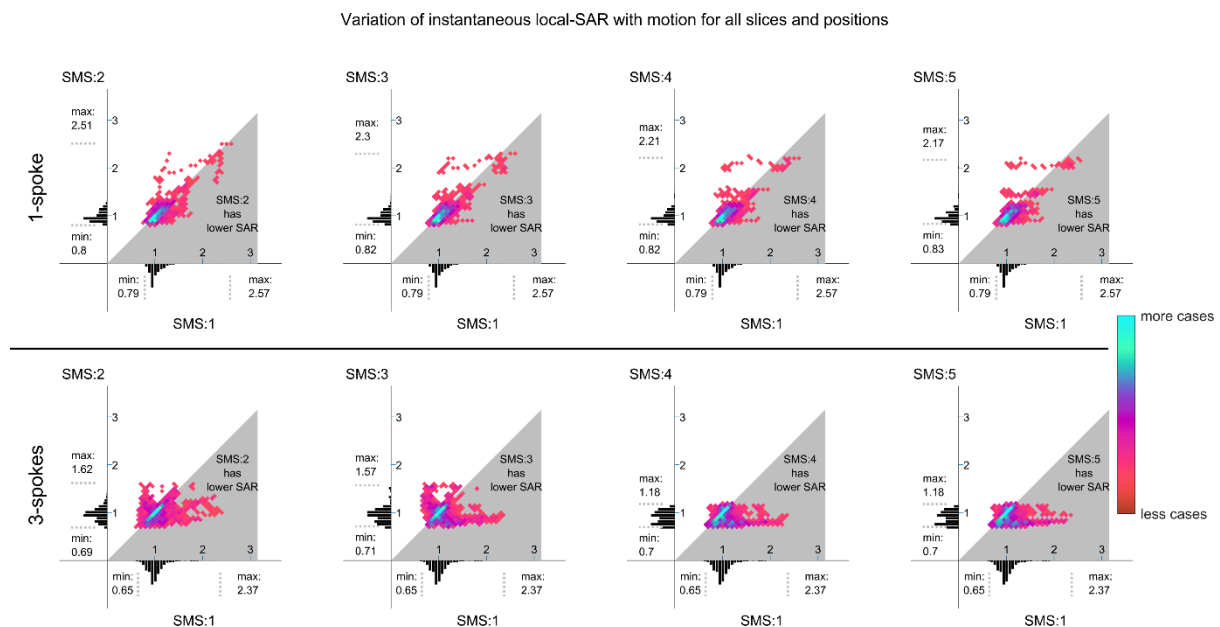
Figure 4: *The variation of peak local-SAR due to patient motion across all off-centre positions and all pulses is compared for different SMS-factors for 1-spoke and 3-spokes pulses. The peak local-SAR at the off-centre positions were normalized with their respective peak local-SAR at the centre. Increasing the SMS-factor from 1 to 5 reduces the motion-sensitivity of local-SAR by 16% for RF shimming (1-spoke pulse), and by 50% for 3-spokes pulses. Intensities: number of cases that fall inside the patches. Histograms: projections onto the axes.*

Discussion

We have investigated the effect of patient motion on local-SAR for simultaneous multi-slice excitation at 7T. The results show that pulses designed with higher SMS-factors are more robust against local SAR changes due to patient motion when compared to pulses with lower SMS-factors. Moreover, increasing the SMS-factor reduced the variation of peak local-SAR throughout the scan when patient motion was not observed.

The local-SAR increased between 18% and 175% across all cases investigated. To ensure patient safety, the effect of motion should be taken into consideration in pulse design, especially for patient populations that may not stay still for extended durations (10,11).
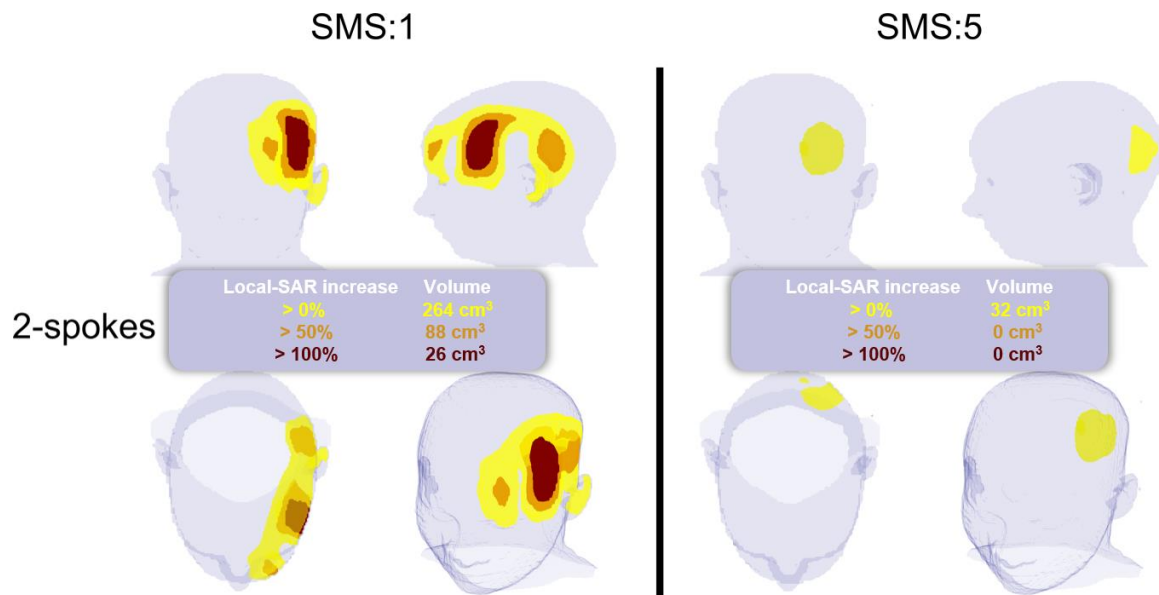
Figure 5: The increase in the local-SAR due to patient motion is compared for the 2-spokes SMS:1 and SMS:5 pulses with maximum local-SAR increase due to motion. For each pulse, the local-SAR at the worst-case position was compared to the peak local-SAR at the centred position. The SMS:1 case yielded a 2.75-fold increase in the local-SAR while the SMS:5 case yielded a 1.38-fold increase. Note that each case is compared against its respective local-SAR at the centred position. Colour scale indicates local-SAR increase; yellow, <50%; orange; 50%-100%; red, >100%.

REFERENCES

1. Feinberg DA, Setsompop K. Ultra-fast MRI of the human brain with simultaneous multi-slice imaging. J Magn Reson 2013;229(0):90-100.
2. Wu X, Schmitter S, Auerbach EJ, Moeller S, Ugurbil K, Van de Moortele PF. Simultaneous multislice multiband parallel radiofrequency excitation with independent slice-specific transmit B1 homogenization. Magn Reson Med 2013;70(3):630-638.
3. Poser BA, Anderson RJ, Guerin B, Setsompop K, Deng W, Mareyam A, Serano P, Wald LL, Stenger VA. Simultaneous multislice excitation by parallel transmission. Magn Reson Med 2014;71(4):1416-1427.
4. Guerin B, Setsompop K, Ye H, Poser BA, Stenger AV, Wald LL. Design of parallel transmission pulses for simultaneous multislice with explicit control for peak power and local specific absorption rate. Magn Reson Med 2015;73(5):1946-1953.
5. Kopanoglu E, Plumley AJD, Erturk A, Deniz CM, Wise RG. Implications of within-scan patient head motion on B1+ homogeneity and Specific Absorption Rate at 7T. Proc. ISMRM 2019; 2019; Montreal, Canada. p 4686. (Proc. ISMRM 2019).
6. Andreas C, Wolfgang K, Eckhart GH, Katharina H, Marcel Z, Esra N, Wolfgang R, Rolf J, Werner B, Ji C, Berthold K, Peter S, Hans-Peter H, Jianxiang S, Michael O, Dominik S, Anthony K, Joshua WG, Niels K. The Virtual Family—development of surface-based anatomical models of two adults and two children for dosimetric simulations. Physics in Medicine & Biology 2010;55(2):N23.
7. Wolf S, Diehl D, Gebhardt M, Mallow J, Speck O. SAR simulations for high-field MRI: how much detail, effort, and accuracy is needed? Magn Reson Med 2013;69(4):1157-1168.
8. Grissom W, Yip CY, Zhang Z, Stenger VA, Fessler JA, Noll DC. Spatial domain method for the design of RF pulses in multicoil parallel excitation. Magn Reson Med 2006;56(3):620-629.
9. Kopanoglu E, Constable RT. Radiofrequency pulse design using nonlinear gradient magnetic fields. Magn Reson Med 2015;74(3):826-839.
10. Malviya S, Voepel-Lewis T, Eldevik OP, Rockwell DT, Wong JH, Tait AR. Sedation and general anaesthesia in children undergoing MRI and CT: adverse events and outcomes. Br J Anaesth 2000;84(6):743-748.
11. Prasher V, Cumella S, Natarajan K, Rolfe E, Shah S, Haque MS. Magnetic resonance imaging, Down's syndrome and Alzheimer's disease: research and clinical implications. J Intellect Disabil Res 2003;47(Pt 2):90-100.